Facies (2009) 55:387–400
DOI 10.1007/s10347-008-0173-1

ORIGINAL ARTICLE

Charophyte-rich microfacies in the Barremian of the Eastern Iberian Chain (Spain)

Hasdrúbal Climent-Domènech · Carles Martín-Closas · Ramon Salas

Received: 17 May 2008 / Accepted: 26 November 2008 / Published online: 18 December 2008

Abstract Non-marine carbonate microfacies based on charophytes are a useful palaeoenvironmental tool that has been poorly developed to date. In the Barremian of the Maestrat Basin (Eastern Iberian Chain), five such microfacies are described and interpreted in terms of sedimentology and palaeoecology: (1) Microfacies of clavatoracean remains are mudstones and wackestones rich in utricles and well-preserved charophyte thalli of the genus *Clavatoraxis*, representing in situ deposition of clavatoracean meadows. (2) Microfacies of filamentous algae and clavatoraceans are mudstones with a high proportion of calcified filaments attributed to cyanobacteria and green algae. This facies may correspond to the open lake benthos. (3) Microfacies of Intraclasts and Charophyte remains are packstones formed on the shores of freshwater lakes or brackish swamps that underwent subaerial desiccation and wave reworking. (4) Microfacies of Porocharacean remains are wackestones and packstones with abundant gyrogonite fragments of genus *Porochara*. They are related to the reworking of a porocharacean meadow in shallow brackish marshes. (5) Microfacies of *Munieria* grambasti Bystricky 1976 fragments are grainstones attributed to the reworking of *Munieria*-dominated meadows. In consequence to these results, a palaeoecological model based on charophyte remains is proposed as a useful tool in carbonate facies analysis.

Keywords Charophyta · Palaeoecology · Non-marine facies analysis · Early Cretaceous · Iberia

H. Climent-Domènech · R. Salas
Departament de Geoquímica, Petrologia i Prospecció Geològica, Facultat de Geologia, Universitat de Barcelona, Barcelona, Catalonia 08028, Spain

C. Martín-Closas (✉)
Departament d'Estratigrafia, Paleontologia i Geociències Marines, Facultat de Geologia, Universitat de Barcelona, Barcelona, Catalonia 08028, Spain
e-mail: cmartinclosas@ub.edu

Introduction

Non-marine carbonate microfacies are usually characterized on the basis of abundant fossil-charophyte remains and related fauna (e.g., ostracodes, freshwater molluscs, vertebrate bones) and flora (e.g., charophytes, cyanobacteria). Lime-mudstones and wackestones rich in charophyte thalli and gyrogonites are, for instance, among the most abundant carbonate lithology of Late Jurassic and Early Cretaceous Purbeck- and Wealden-like facies in the Tethyan Domain. The general view is that these types of facies are much more monotonous and less diverse than their shallow-marine counterparts and therefore little attention is paid to them in most synthetic studies of carbonate microfacies analysis (e.g., Flügel 2004). Even if the first assertion may be true in part, it is no less true that only a few detailed studies deal with the recognition of non-marine components, especially thalli and reproductive organs of charophytes, in thin sections of carbonate rocks. However, the morphology, anatomy, palaeoecology, and evolution aspects of fossil charophytes are quite well known (Martín-Closas 2003; Feist et al. 2005), which assists the description of new carbonate microfacies based on this land–plant related phylum. In addition, the taphonomic and palaeoecological characterization of charophyte-rich facies gives new clues for the palaeoenvironmental interpretation of non-marine carbonate rocks, which is the main objective of the present study.

Material and methods

Twenty-five carbonate rock samples were selected by their abundance in non-marine components after systematic sampling of the Creu del Vilar stratigraphic section in the Barremian of Aiguaviva, Castelló Province, Spain. Thin sections, about 10–15 μm thick, were prepared after the oriented samples were cut perpendicular to the stratification. Samples were studied and components of the microfacies were counted under conventional optical microscopy at 40× magnification. Point-quadrat counting was performed with a net of 1 mm^2 on a total surface of 5 cm^2 per thin section, following the method of Perrin et al. (1995). In total, 500 points per thin section were counted and their skeletal composition was determined. Rarefaction curves showed that after 400 points had been counted, the percentages of different components remained stable in all thin sections. These percentages constituted the database that was later analyzed by cluster analysis with the PAST (Paleontological Statistics) software, created by Hammer and Harper (2006).

Geological and stratigraphic settings

The study area, located near the village of Aiguaviva, northwest of the Castelló province (eastern Spain), belongs to the Linking Zone between the Iberian Chain and the Catalan Coastal Chain (Fig. 1). This area is structurally characterized by a complex of Alpine compressive structures largely oriented east to west, intermediary between the Iberian NW–SE structures and the Catalan NE–SW structures (Fig. 2). These structures represent the Late Eocene and Oligocene inversion of Mesozoic normal faults, which bounded a number of parallel half-grabens that subsided from the Late Permian to the Maastrichtian.

During the Late Jurassic to Early Cretaceous rifting stage as defined by Salas and Casas (1993), the study area belonged to the eastern part of La Salzedella Basin, which was in turn part of a larger system of basins that make up the Maestrat Basin. In these basins, the stratigraphic succession is characterized by the accumulation of up to 5,000 m of shallow-marine and non-marine carbonates and estuarine clastics organized in 13 depositional sequences. The onset of the Late Jurassic–Lower Cretaceous rifting stage was in parallel with a global relative rise in sea level. Thus, the Oxfordian sequence (J8 of Salas et al. 2001) is formed by up to 50 m of shallow carbonate ramp facies rich in sponges (Iàtova Fm), whereas in the Kimmeridgian (sequence J9 of Salas et al. 2001) the sedimentation included up to 300 m of basin anoxic marls rich in hydrocarbons (Mas d'Ascla Fm). These deeper facies passed laterally to a relatively reduced thickness of shallower carbonate ramp facies (Polpís Fm). The Tithonian-Berriasian sequence (J10 of Salas et al. 2001) was mainly formed in the basin by shallow carbonate platforms with

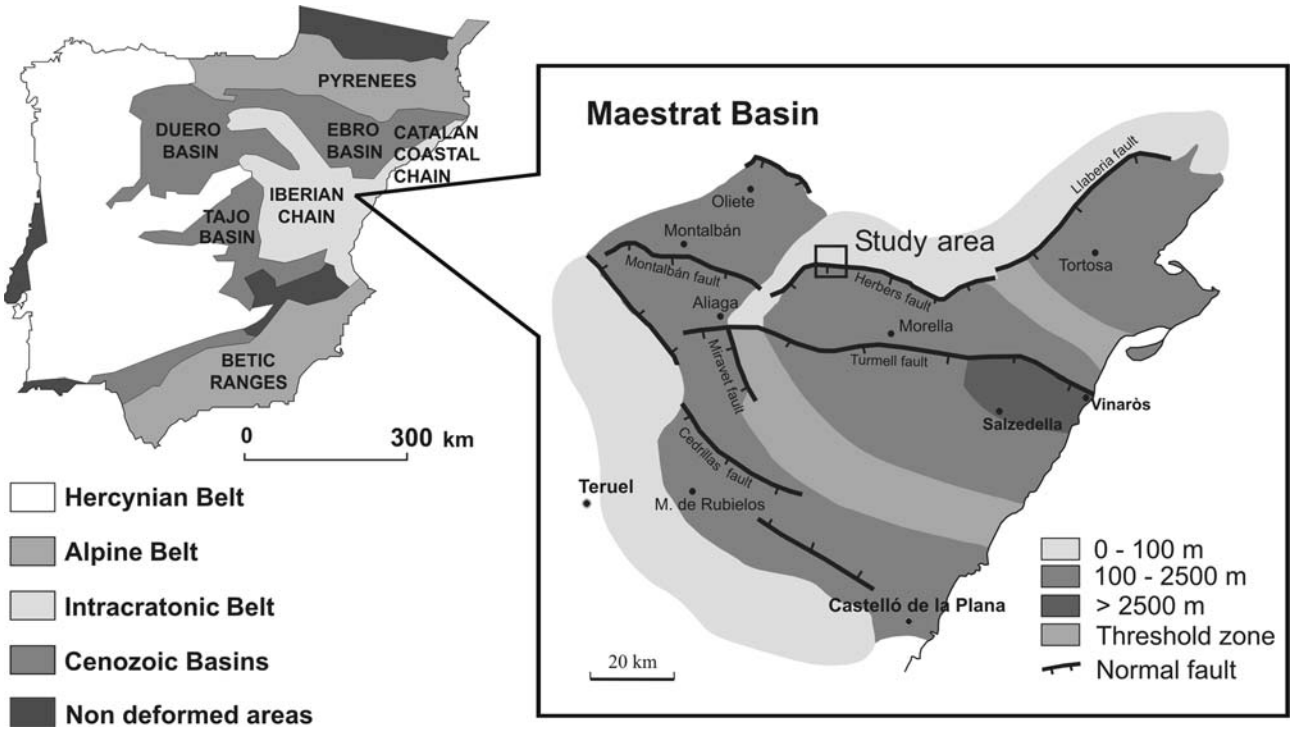

Fig. 1 Geological setting of the study area in the Maestrat Basin, Eastern Iberian Chain

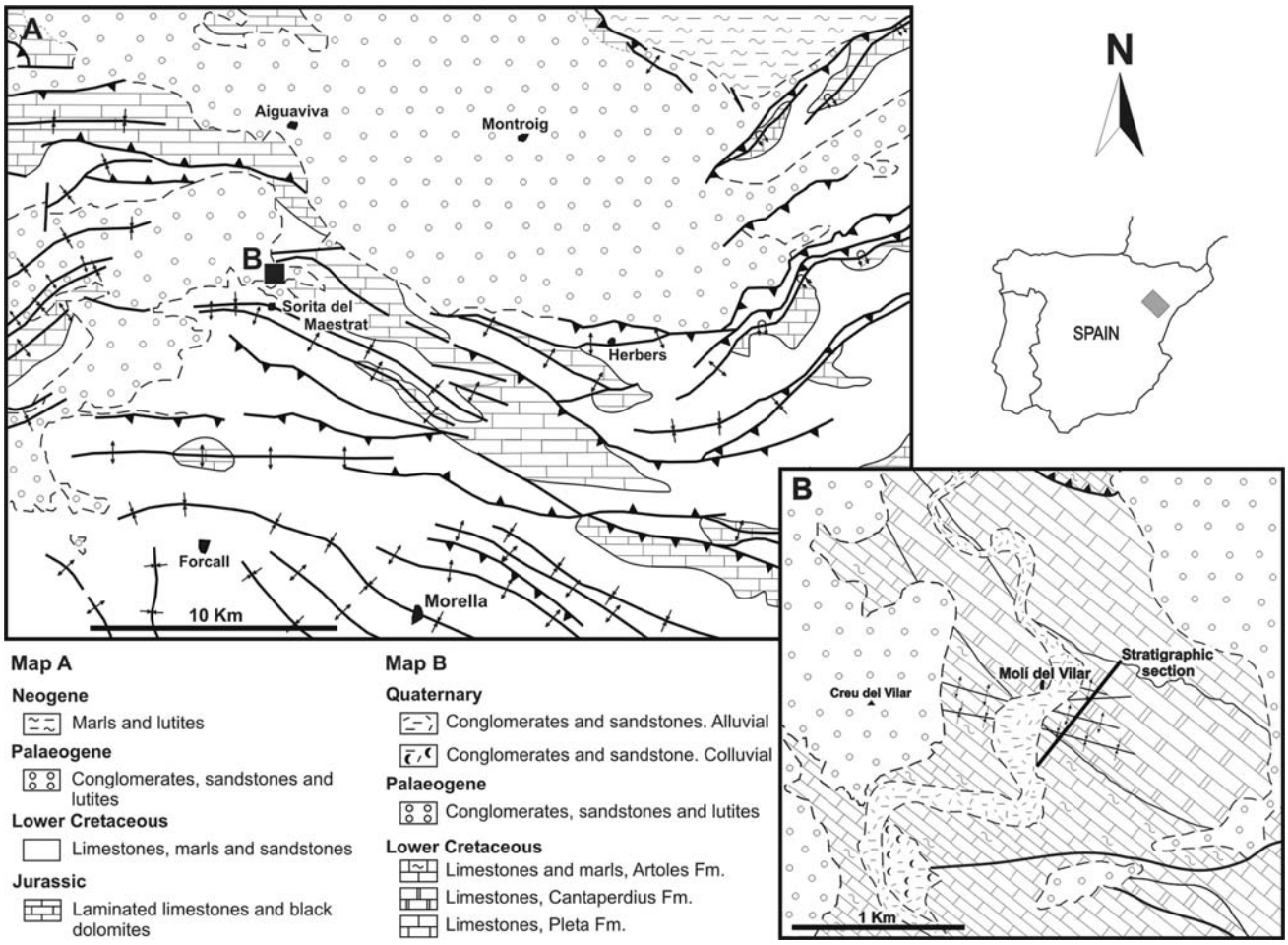

Fig. 2 General geographical location and geological sketch of the study area (**a**) and detailed location of the studied section (**b**), near the border between the folded and thrusted Iberian Chain and the Cenozoic Ebro Basin

extensive intertidal flats bounded by oolithic–bioclastic shoals (La Pleta Fm). These deposits change to deeper *Calpionella*-limestones, up to 1,000 m thick, towards the basin center. The Upper Berriasian to Barremian sequences (K1.1–K1.7 of Salas et al. 2001), with a thickness of up to 1,500 m, are characterized in the basin margins by lacustrine to palustrine limestone and marls, rich in charophytes, grading from freshwater to brackish and finally to marine marginal facies. In the Barremian (sequences K1.4–K1.7), these rocks were deposited in a well-developed wetland system, the Cantaperdius Fm, which is the subject of the present study, linked seawards to estuaries. The non-marine facies passed laterally to shallow-marine carbonate platforms rich in molluscs and calcareous algae, mainly cyanobacteria, dasycladaleans and red algae, protected by oolithic–bioclastic shoals and coralgal build-ups. During the Barremian, these facies belonged to the Artoles Fm. In the Lowermost Aptian (sequence K1.8 of Salas et al. 2001), the sedimentation was characterized by a well-developed deltaic complex with dominant mud-flat deposits rich in dinosaur remains, mainly iguanodontid (red beds of the Morella Fm). In contrast, the rest of the Aptian (sequences K1.8–K1.9) is represented by relatively small shallow-marine carbonate platforms rich in rudists and marine calcareous algae, changing towards the sea, to deeper facies of marls with orbitolinids and ammonites. The Aptian deposits are up to 1,200 m thick. Finally, the Lower–Middle Albian depositional sequence (K1.10 of Salas et al. 2001) consists of up to 500 m of siliciclastic deposits belonging to a very large deltaic system affected by tides and with a significant development of brown coal and abundant cheirolepidiaceous conifer remains in the upper delta plain (Escucha Fm).

The section studied at Creu del Vilar shows a relatively complete record of the Barremian sequences K1.4–K1.7 in the basin margins (Fig. 3). The Barremian succession was deposited unconformably on the Tithonian–Berriasian laminated tidal limestones of La Pleta Fm and is covered unconformably by Paleogene conglomerate and sandstone. The lower part of the succession is dominated by freshwater grey to yellow limestone and marls of the Cantaperdius Fm. Four marine wedges, progressively thicker towards the

top, represent a clear transgressive trend, which was common in the whole basin during the Barremian. The upper part of the section is exclusively formed by shallow-marine limestone and marls of the Artoles Fm. The whole section records a complete biostratigraphic succession of Barremian charophyte assemblages. The main part of the Cantaperdius Fm (first 350 m of the succession) includes assemblages formed by *Atopochara trivolvis* var. *triquetra* (Grambast 1968) Martín-Closas, *Globator maillardii* var. *trochiliscoides* (Grambast 1966) Martín-Closas 1996 (typical morphotype), *Ascidiella triquetra* (Grambast 1969) Martín-Closas 1996, *Clavator harrisii* Peck 1941, *Clavator calcitrapus* (Grambast 1969) Martin-Closas ex Schudack 1993 and *Hemiclavator neimongolensis posticecaptus* (Martín-Closas and Grambast-Fessard 1986) Martín-Closas 1996, which are characteristic species of the Triquetra Biozone of Riveline et al. (1996), Early Barremian in age. The upper part of the non-marine succession shows assemblages of *Globator maillardii* var. *trochiliscoides* (Grambast 1966) Martín-Closas 1996 (advanced morphotype), *Clavator harrisii* Peck 1941 and *Hemiclavator neimongolensis* var. *neimongolensis* Wang and Lu 1982, belonging to the Cruciata-Paucibracteatus biozone of Martín-Closas et al. (2009), which, in the stratigraphic context of the Artoles Fm, indicates a Late Barremian age.

In sedimentological terms, the non-marine deposits of the Cantaperdius and Artoles Fms at Creu del Vilar are organized in a number of smaller shallowing-upwards cycles, a few meters thick. Two types of cycles were recognized depending on their palaeoenvironmental setting:

a) Cycles of freshwater lake deposits are formed by a basal term of marls and lime-mudstones with rare charophyte remains (mainly clavatoracean utricles and thalli) and limnic ostracodes. In microfacies analysis, calcified algal filaments were also a characteristic component. The upper term of the cycle was formed by wackestones-packstones showing, in addition to rich charophyte remains and ostracodes, abundant intraclasts (black and white pebbles), color mottling, and sometimes rootlet casts and marks. This type of cycle is attributed to infilling sequences of highly alkaline lakes, which graded upwards from deeper lacustrine facies to lakeshore or palustrine deposits with reworking of exposed mud-cracks and edaphic features.
b) Cycles of brackish marsh deposits are formed by a basal term of wackestones-packstones with porocharacean gyrogonites, small benthic foraminifera (mainly lituolids and milolids), dasycladaleans, ostracodes, molluscs and vertebrate eggshells (probably from turtles). Some horizons show a peletoidal fabric. Siliciclastic sand may be abundant in the basal term of some cycles, which, in addition, are devoid of charophyte remains and show instead an assemblage of miliolids, serpulids, ostreids, gastropods, and ostracodes. The upper term is formed by packstones with a diverse assemblage of marine skeletal remains, such as small benthic foraminifera, echinoids, bryozoans, and red and green algae (halimedaceans and dasycladales). A significant amount of sand may also be present in some layers of this facies. This type of cycle is attributed to deposition in brackish marshes and lagoons covered by nearshore marine facies in a transgressive context.

This study deals with the limestones rich in charophyte remains, i.e., limestone of the freshwater type cycles and the basal term of the brackish marsh cycles.

Results

Definition of components

Ten different categories of components were taken into account: (1) Thalli of the genus *Clavatoraxis* (Figs. 4a–d), which bear characteristic spine-cell rosettes (Martín-Closas and Diéguez 1998). (2) Thalli of the genus *Charaxis* (Figs. 4e–f), which display the usual *Chara*-like cortication of internodes. (3) Thalli of *Munieria grambasti* Bystrický 1976 (Figs. 5a–b), which are characterized in thin section by a particular pattern of calcification limited to the intercellular space between cortical and internodal cells. As a result, the transversal section of internodes is shaped like a toothed wheel (Fig. 5b). These types of thalli were related to dasycladales by some authors, such as Feist et al. (2003), while others, including Schudack (1993) and Martín-Closas (2000), attributed them to charophytes, probably clavatoraceans. *Munieria* internodes display a key feature of charophytes, which is the interfingering of cortical cells coming from successive nodes in the middle part of the internode. (4) Clavatoracean utricles are distinct in their bottle-shaped section (Figs. 5c–d). Two types of utricles were found; atopocharoidean utricles lack a calcified gyrogonite (Fig. 5c), while clavatoroidean utricles coat poorly-calcified gyrogonites (Fig. 5d). (5) *Porochara* gyrogonites (Figs. 5e–f), characterized by their rounded section, strong calcification of spiral cells, usually showing the internal Y-structure described by Feist and Grambast-Fessard (1984), and a multipartite basal plate visible in thin sections. (6) Calcified filaments without internal compartmentalization (Figs. 6a–b). Two types of filaments were recognized from their diameters but were not separated in the data matrix as they are generally associated with each other. Small filaments about 20 μm across may belong to cyanobacteria. Some of these were organized in bundles and were attributed to the genus *Girvanella* (Fig. 6a), which is considered to be of

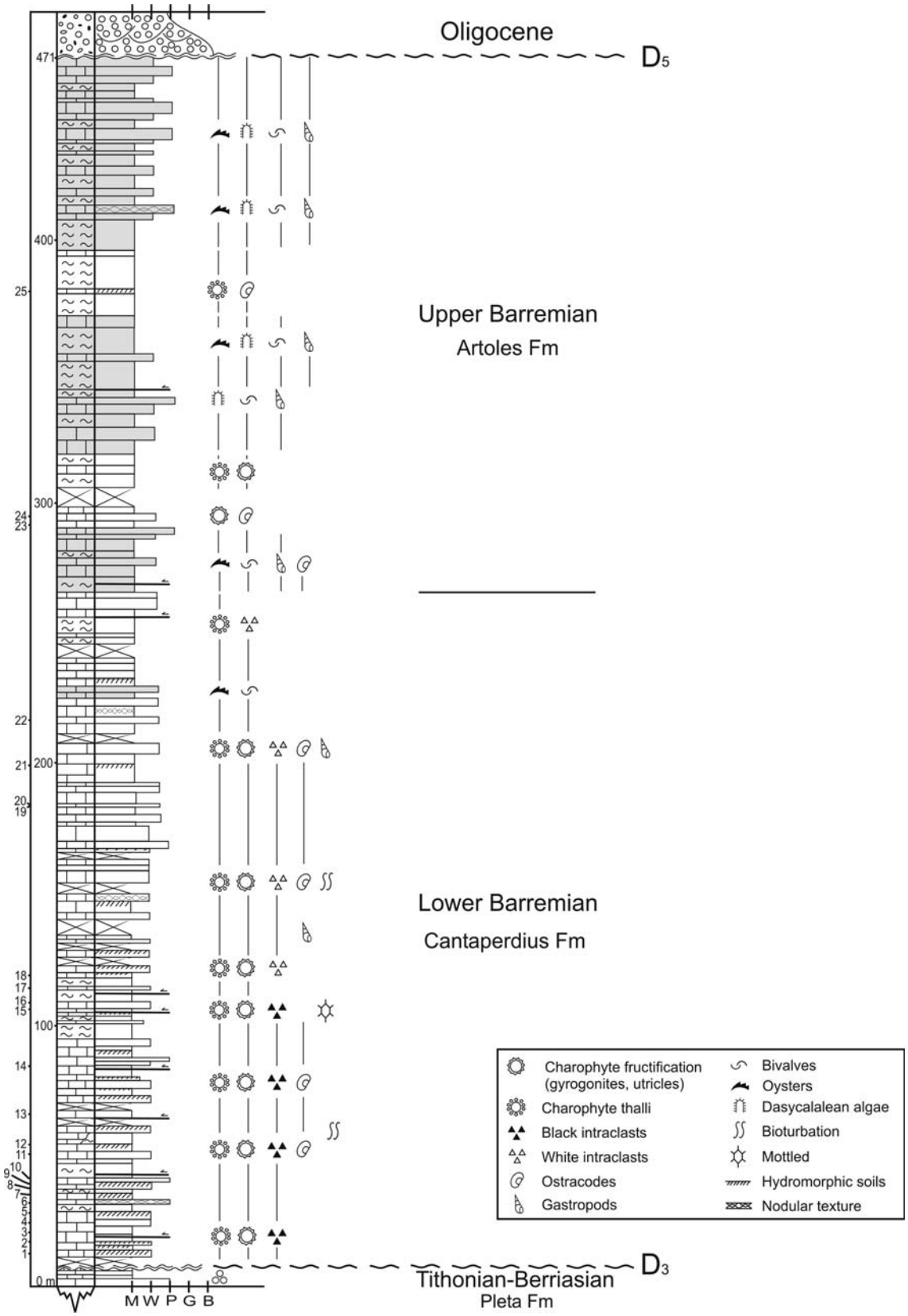

Fig. 3 Stratigraphic section of Creu del Vilar with location of samples 1–25 studied. Marine-influenced terms of the section are *shaded*

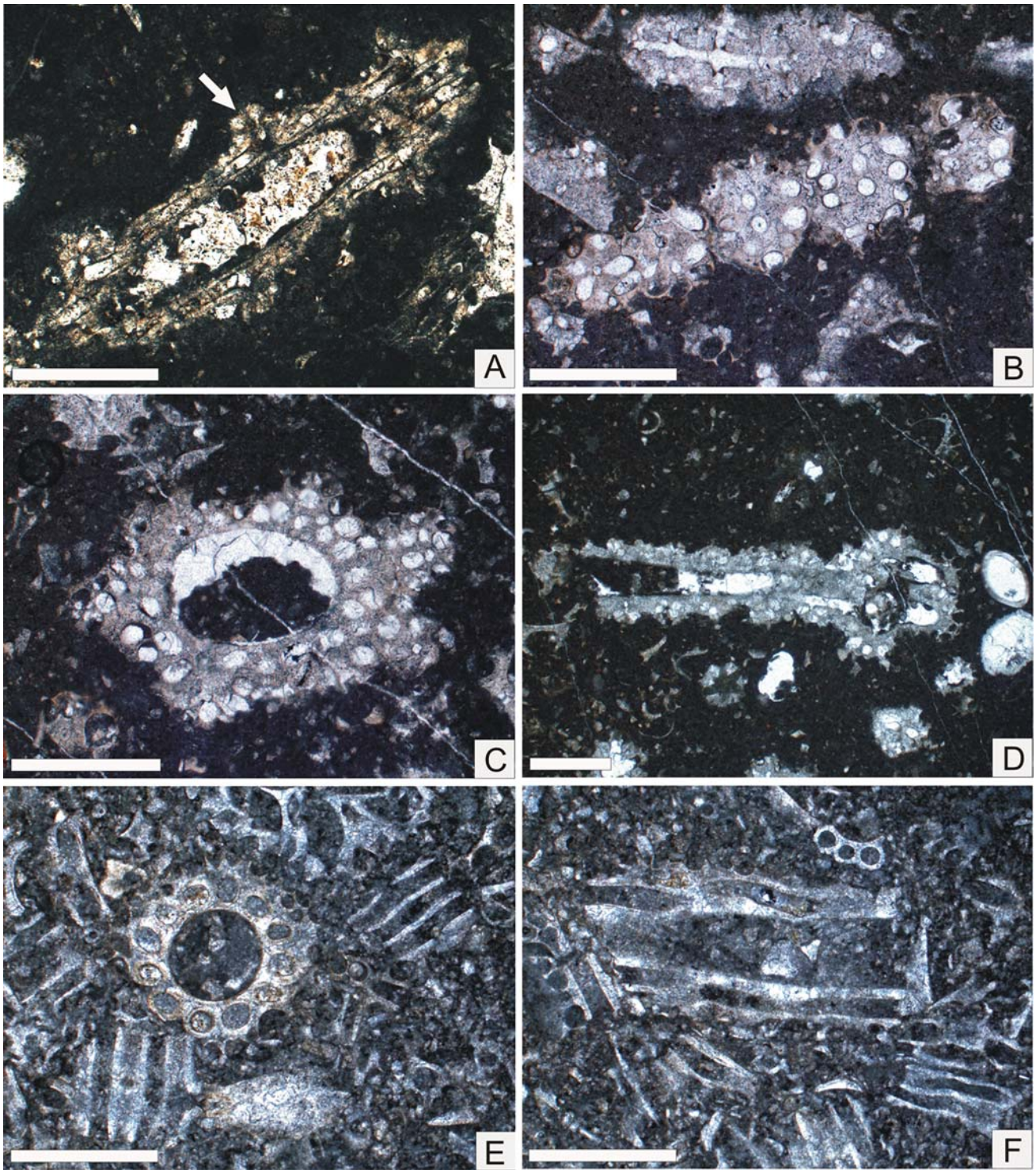

Fig. 4 Components distinguished in the microfacies analysis. **a** Oblique section of a *Clavatoraxis* thallus with characteristic spine-cell rosettes (*arrows*); sample 2. **b** Tangential section through a phylloid (last-order branchlet) of *Clavatoraxis* showing five spine-cell rosettes; sample 6. **c** Cross section of a *Clavatoraxis* thallus; sample 6. **d** Longitudinal section of a *Clavatoraxis* internode and adjacent node, sample 6. **e** Cross section of a *Charaxis* thallus, sample 20. **f** Longitudinal section through a *Charaxis* internode; sample 20. *Scale bars* equal 500 µm

cyanobacterial affinity (Riding 1991). Large calcified filaments are ca. 100 µm across and may belong to green algae or ecorticate charophytes (Fig. 6b), such as *Paleonitella*. Surface features, not available in thin sections, are necessary to confirm the latter attribution. (7) Benthic foraminifera, in most cases belonging to lituolids or miliolids. (8) Ostracod shells. (9) Vertebrate eggshells (Fig. 6d), which were attributed to turtles on the basis of their thickness and

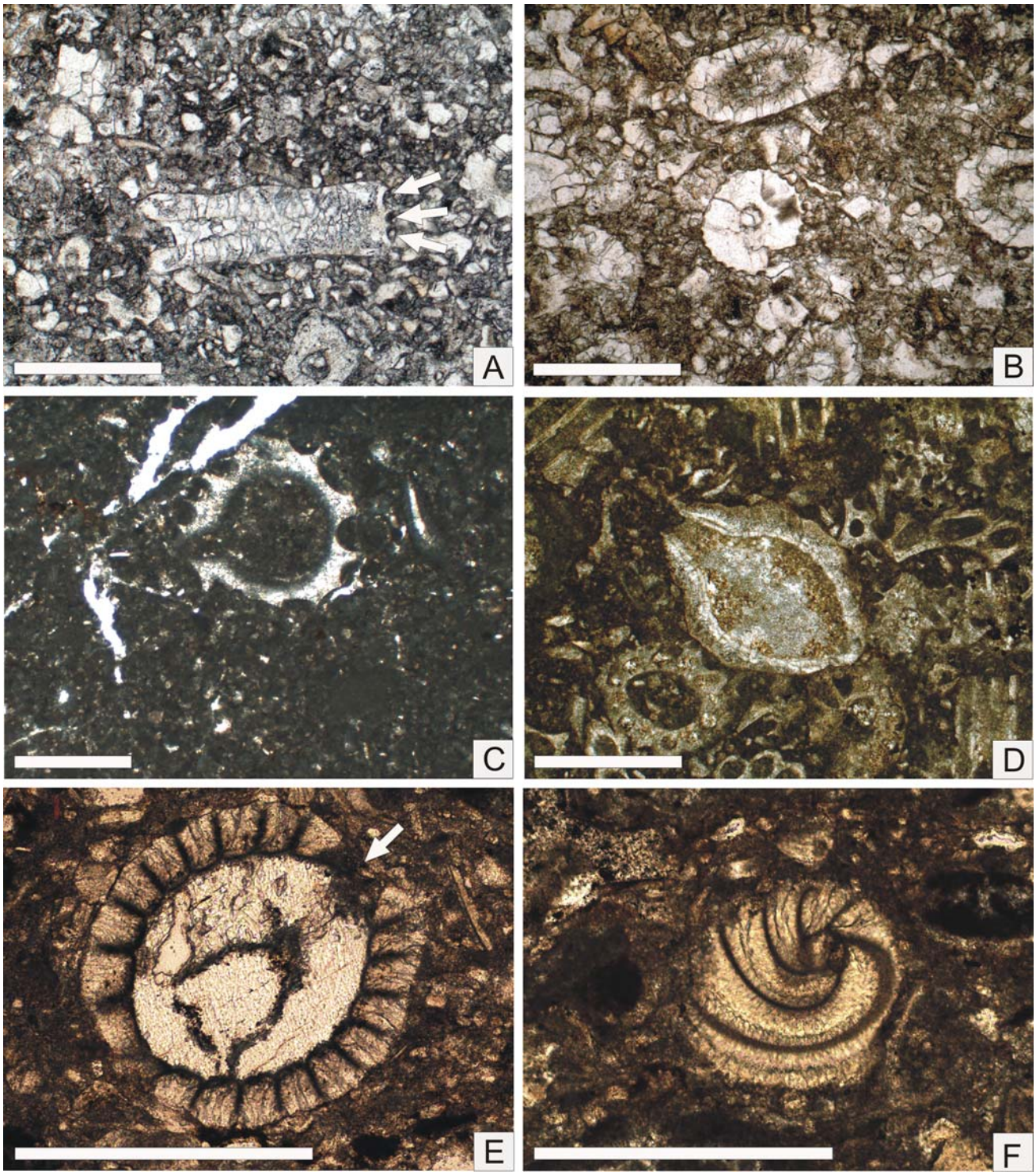

Fig. 5 Components distinguished in the microfacies analysis (continued). **a** Longitudinal section through an internode of *Munieria*, showing the scars of three nodal cells (*arrows*); sample 19. **b** Cross section through internode of *Munieria*, with characteristic crenulations corresponding to the internal side of cortical cells; sample 19. **c** Longitudinal section of an atopocharoidean utricle, probably belonging to *Atopochara*, showing the characteristic bottle-shaped cast of the oogonium (not calcified); sample 17. **d** Longitudinal section of a clavatoroidean utricle upon the calcified gyrogonite; sample 16. **e** Longitudinal section of a porocharacean gyrogonite showing Y-calcification and apical pore (*arrow*), sample 24. **f** Tangential section through the internal part of base of a *Porochara* gyrogonite, showing a multipartite basal plate, sample 24. *Scale bars* equal 500 μm

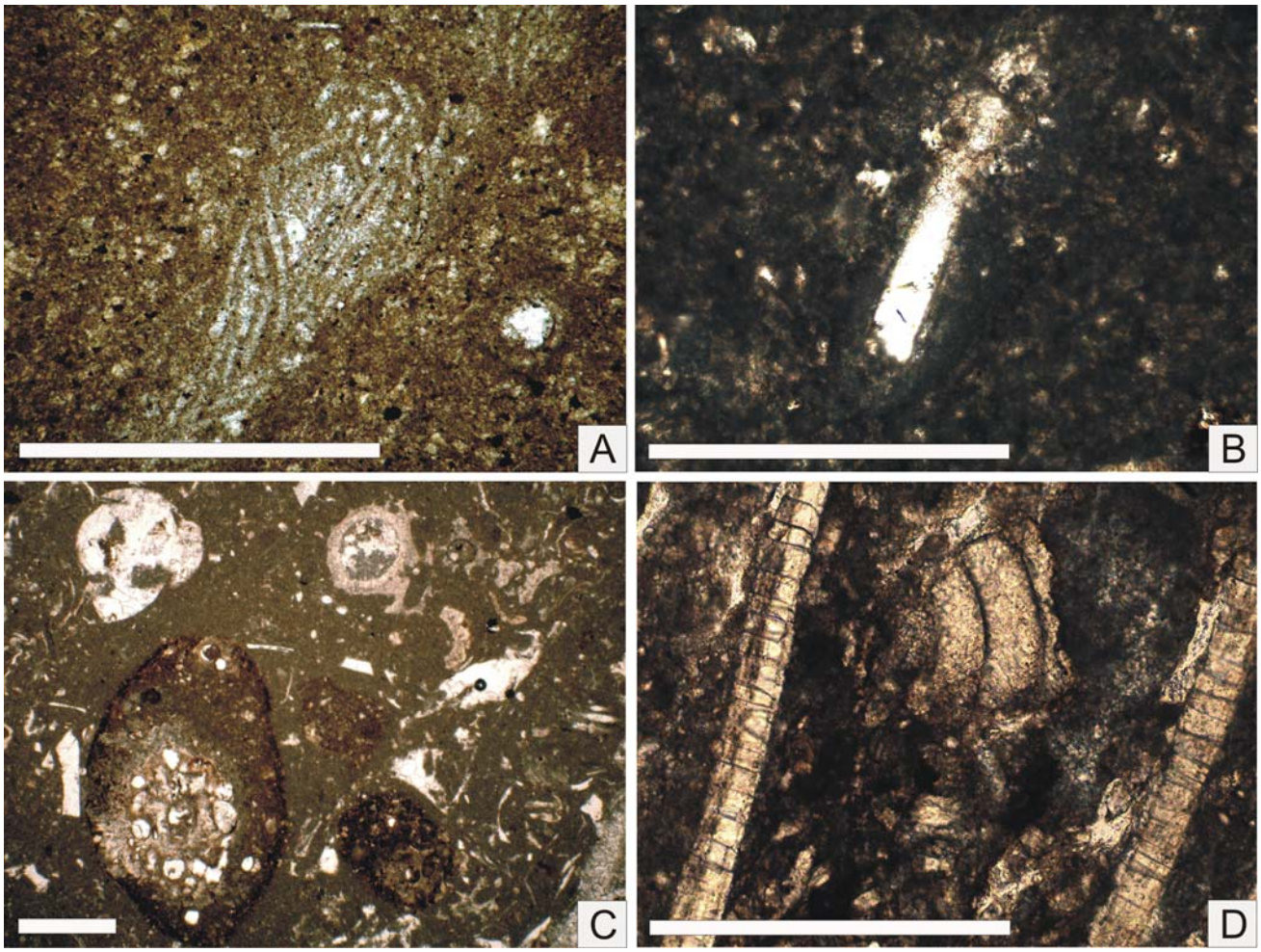

Fig. 6 Components distinguished in the microfacies analysis (continued). **a** Bundle of *Girvanella*, formed by filaments of cyanobacterial affinity, sample 15. **b** Oblique section through a large filament attributed to green algae or ecorticated charophytes, sample 17. **c** Intraclasts showing a similar composition to surrounding sediment; sample 22. **d** Section through vertebrate eggshells attributed to turtles, sample 24. *Scale bars* equal 500 μm

internal structure. (10) Intraclasts are mainly black or white pebbles showing composition and texture similar to the surrounding sediment (Fig. 6c).

In some of these categories of components, a distinction was made, for taphonomic purposes, between complete and fragmentary remains. Two additional categories correspond to lime-mud and undetermined bioclasts. The latter included up to 40% of the total number of points counted in some samples and correspond to small bioclasts of undetermined affinity. This category was not taken into account in the cluster analysis since it masked the groups defined by well-known components and because the information provided by this variable is already contained in the determination of the rock fabric.

Definition of microfacies

Microfacies considered in this study were obtained from cluster analysis of the database matrix provided in Table 1, which resulted from the point-quadrat counting of components in thin sections, as explained in the Materials and methods section. From all the algorithms and similarity indexes provided for clustering by the PAST (Paleontological Statistics) software of Hammer and Harper (2006), the Paired Group algorithm and the Horn method gave the highest correlation coefficient (0.95). Other algorithms and abundance similarity measures were checked and discarded due to their lower correlation coefficients (0.70–0.85). The dendrogram resulting from the application of this analysis is shown in Fig. 7. The samples analyzed are grouped in five distinct assemblages. Three main groups (A–C) are characterized by particular components, *Munieria*–type thalli for group A, porocharacean gyrogonites for group B, and clavatoracean remains (mainly utricles and *Clavator-axis* type thalli) for group C, which constitutes the crown group of the samples analyzed. Within this crown group, three subgroups are distinguished. The most basal of them

Table 1 Data matrix of components obtained from point-quadrat counting of the thin sections studied

Sample	Microfacies	Fabric	Components (%)													
			MUD	CHAR	CLAV	UTRI	PORO	PORF	MUNI	MUNF	FILA	INTR	FORA	EGGS	OSTR	INDET
20	C_3	Packstone	36.2	25.2	12.2	4.8	0.6	0	0.2	0	0	0	0	0	0	20.8
1	C_3	Wackestone	61	4.2	2	1.2	0.2	0	2.4	0	0	0	0	0	1.2	27.8
12	C_3	Packstone	56.2	14.2	5.6	0.6	1.2	0	0	0	0	0	0	0	1.4	20.8
10	C_3	Wackestone	63.6	8	4.6	0.4	0.4	0	0	0	2.2	0	0	0	2.8	18
2	C_3	Packstone	54.6	20.2	3	0.2	0	0	0	0	1.2	0	0	0	0.8	20
4	C_3	Wackestone	51.4	11.6	4.2	3.4	0	0	1.2	0	0	0	0	0	1.8	26.4
9	C_3	Wackestone	55.6	20.2	2	1	0	0	0	0	1	0	0	0	2.6	17.6
18	C_3	Packstone	38.8	12.8	0.4	4.6	0	0	0	0	0	0	0	0	2.6	40.8
3	C_3	Wackestone	41	19.4	3.4	1.8	0	0	0	0	0.6	0	0	0	1.2	32.6
21	C_3	Wackestone	50.6	8.4	9.4	0.8	0	0	0	0	6.2	0	0	0	3	21.6
15	C_3	Wackestone	44.6	7.2	12.2	0.4	0	0	0	0	5.6	0	0	0	1.6	28.4
8	C_3	Wackestone	57.6	5.8	11.6	0.8	2	0	0	0	1.8	0	0	0	5.4	15
14	C_3	Wackestone	54.4	8.6	7	1	0.8	0	0.6	0	2.4	0	0	0	3.6	21.6
5	C_3	Wackestone	50	4.8	14	1.6	0	0	1.2	0	0.6	0	0	0	1.2	26.6
6	C_3	Wackestone	36.6	7.4	27.2	0	0	0	0	0	0	0	0	0	2.8	26
7	C_3	Wacke-Packstone	43.2	9.6	15.2	1	0	0	0	0	0	0	0	0	1	30
16	C_3	Wacke-Packstone	41	18	14.8	1.2	0	0	0	0	0	0	0	0	2	23
25	C_2	Mudstone	62.2	6.6	1.2	1.8	0	0	0	0	10.6	0	0	0	5	12.6
23	C_2	Mudstone	46.4	11.4	0	2.2	0	0	0	0	16.8	0	0	0	2.6	20.6
17	C_2	Wackestone	58.2	8.2	0	1.2	0	0	0	0	8.4	7.6	0	0	0.8	15.6
22	C_1	Packstone	39	10.4	0	3.8	0	0	0	0	0	13.4	4	0.4	4.4	24.6
11	B	Wackestone	37	0	0	0	2.4	16.4	0	0	0	0	16.2	5.6	0.4	22
24	B	Wackestone	31	0.4	0	0	3.2	16	0	0	0	0	18.2	11.2	0.6	19.4
19	A	Grainstone	23.4	0	0	0.8	0	0	26.2	49.2	0	0	0	0	0.4	0
13	A	Grainstone	41.6	1.8	0	0	0.6	0	5.4	46.6	0	0	0	0	4	0

MUD: micrite, *CLAV*: thalli of *Clavatoraxis*, *CHAR*: thalli of *Charaxis*, *UTRI*: clavatoracean utricles, *PORO*: porocharacean gyrogonites, *PORF*: fragments of porocharacean gyrogonites, *MUNI*: thalli of *Munieria grambasti*, *MUNF*: fragments of *Munieria grambasti*, *FILA*: calcified algal filaments, *INTR*: intraclasts, *FORA*: small benthic foraminifera, *EGGS*: vertebrate eggshell fragments, *OSTR*: ostracodes, *INDET*: undetermined bioclasts

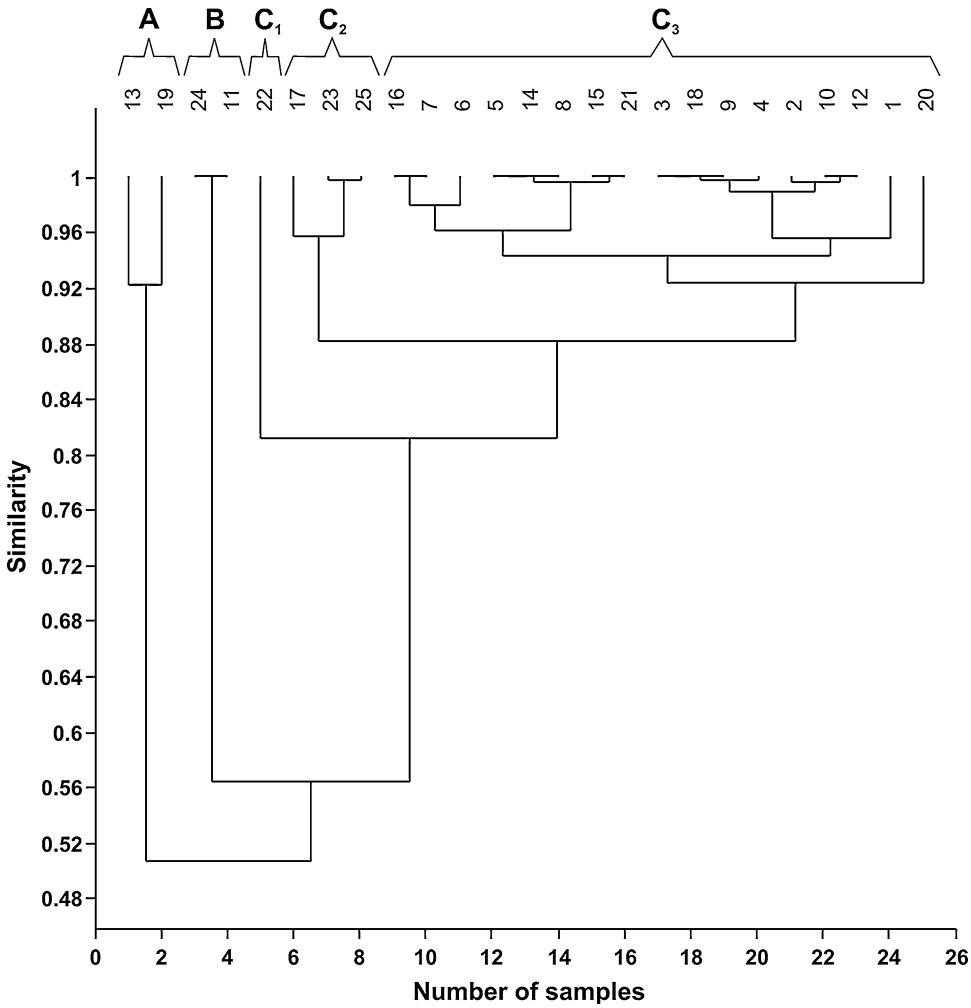

Fig. 7 Dendrogram obtained from cluster analysis of previous data matrix (Table 1) by the Paired Group algorithm and Horn method

(group C_1) is characterized by the abundance of intraclasts in addition to clavatoracean remains. The second branch (group C_2) includes samples with abundant calcified filaments. Finally, the group standing out the most (C_3) includes a large number of closely related samples, characterized by their abundant clavatoracean remains. In the next section, the five groups A, B, C_1, C_2 and C_3 are described and interpreted in terms of palaeoecology.

Description and interpretation of microfacies

Microfacies of clavatoracean remains

This facies consists of wackestones and packstones, 20 cm–1.2 m thick, which in the field are yellowish and may show color mottling and rootlet traces. It corresponds to group C_3 of the dendrogram, which includes most of the samples studied. The microfacies is characterized by abundant clavatoracean remains with a few other skeletal components. Charophyte thalli account for up to 40% of the counted points, usually between 20 and 35% (Fig. 8a). These thalli correspond to the form-genera *Clavatoraxis* and *Charaxis* (Fig. 4), which belong most probably to clavatoracean charophytes (Martín-Closas and Diéguez 1998). Clavatoracean utricles may represent up to 5% of the components counted. Some samples contain a similar amount of ostracod shells. Points that represent lime-mud are very significant and amount to up to 55% of the total. Most of the charophyte thalli are well preserved; they include large portions of internodes, sometimes with nodes and articulated branchlets, suggesting that they were produced by plants growing at the deposition site, or suffering only short and gentle lateral transport before deposition. Some parts of the thalli were biodegraded in situ and show a pelletal fabric within the digested parts, which suggests that the deposition place was in a well-oxygenated part of the lake. This facies is attributed to deposition within a charophyte meadow in the shallower, better oxygenated and illuminated parts of the lake. In sample 18, the rock included up to 40% of undetermined bioclasts, which probably represents small crushed remains of calcified charophyte thalli. The origin of these bioclasts lies in the stronger reworking of charophyte remains on the more energetic lakeshores.

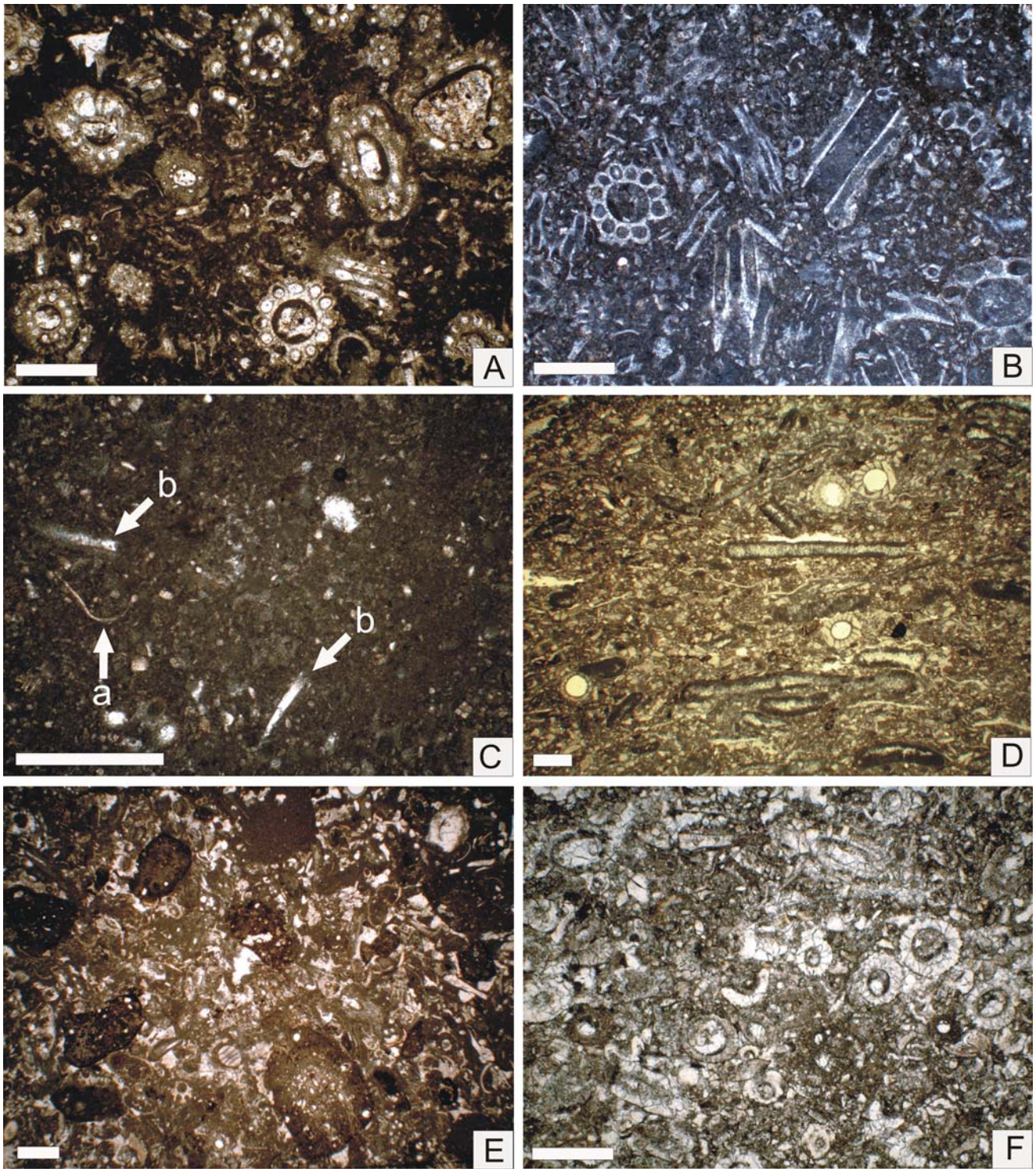

Fig. 8 Microfacies distinguished in this study. **a** Microfacies of clavatoracean remains showing abundant sections of *Clavatoraxis*; sample 16. **b** Microfacies of clavatoracean remains showing abundant sections of *Charaxis*; sample 20. **c** Microfacies of filamentous algae and clavatoraceans showing sections of small cyanobacterial-like filaments (*arrow a*) and larger filaments of eukaryotic algae (*arrow b*); sample 23. **d** Microfacies of porocharacean remains showing sections of gyrogonites and elongated sections of lituolid foraminifera; sample 24. **e** Microfacies of charophyte remains and Intraclasts; sample 22. **f** Microfacies of *Munieria*, sample 19. *Scale bars* equal 500 μm

Facies of filamentous algae and clavatoraceans

This facies corresponds to group C_2 (Fig. 7), which is formed by samples 17, 23, and 25. They are grey to yellowish lime-mudstones and wackestones, 20 cm–1 m thick, sometimes associated with grey marls (see Fig. 8c). In terms of microfacies, this group is defined by its abundance of calcified filaments, which may represent up to 17% of the total points counted. Charophyte remains (clavatoracean thalli and utricules) and ostracodes are less frequent. The two types of filaments described above, belonging to cyanobacteria and green algae, respectively, are always found associated. The accumulation of filaments may produce diffuse lamination that is only visible in thin section. This lamination suggests that the calcified cyanobacterial-like filaments could develop into microbial mats. Unlike calcified filaments, corticate charophyte thalli were less well preserved and usually corresponded to small portions of internodes, which suggests that they underwent some type of transport before deposition. The plant assemblage, dominated by cyanobacteria and filamentous green algae in the absence of in situ macrophytes, suggests that the benthic community was more limited in its growth than previous facies. The fabric, which is dominated by lime-mudstones, points to greater lake depth. In conclusion, this facies is attributed to deposition in deeper and less-illuminated parts of the lake.

Facies of charophyte remains and intraclasts

This facies corresponds to group C_1 and is represented by sample 22, with more than 13% of intraclasts (Figs. 7, 8). Another sample rich in intraclasts (sample 17) is ranged in cluster analysis with group C_2 due to its richness in calcified filaments (see Fig. 8e). In the outcrop, the rock generally stands out due to its distinctive pattern of colored intraclasts on a greyish wackestone to packstone matrix. These facies may be associated with rootlet casts and marks. In microfacies analysis, the intraclasts are less distinctive but still easy to recognize because of their darkening, sharp outline, and differences in fabric. Depending on the sample studied, the skeletal components of the microfacies are intermediate between those of the neighboring groups (B or C_2–C_3). Sample 17 shares with groups C_2–C_3 the abundance in charophyte remains (more than 10% of charophyte thalli and almost 4% of clavatoracean utricles), while sample 22 contains some of the components of group B, such as benthic foraminifera, vertebrate eggshell remains, and rare porocharacean gyrogonites. Charophyte thalli are usually small portions of internodes. Utricles and gyrogonites may be broken. This, along with the abundance of intraclasts, indicates that this facies was deposited on the shores of lakes or marshes submitted to significant wave action and reworking of desiccated mud-cracks. Depending on the differences in facies between the clasts and the matrix deposited after reworking, one should be able to decide the environmental character of pre and post-reworking depositional setting. This accounts for the separation of the samples of this microfacies in two groups of the dendrogram.

Facies of porocharacean remains

This facies is formed by light-colored wackestones with abundant porocharacean gyrogonites (group B in Fig. 7). In the field it occurs in the basal terms of brackish marsh cycles (Fig. 8d). Gyrogonites of genus *Porochara* represent up to 16% of total components and were identified in thin section by their large apical pore, calcification in a Y-pattern and multipartite basal plate (Figs. 5e–f). In the Early Cretaceous, the presence of homogeneous populations of porocharaceans is considered indicative of a brackish environment (Martín-Closas and Grambast-Fessard 1986; Mojon 1989; Schudack 1993). Other components of this facies are abundant benthic foraminifera, mainly lituolids and miliolids (up to 18%) and vertebrate eggshell fragments (up to 11%), probably belonging to turtles. Charophyte thalli and ostracodes are absent or occur in small proportions. Some of the gyrogonites are broken, suggesting that fragmentation occurred during transport. The palaeobiological assemblage and the sedimentological context enable us to relate this facies to deposition of porocharacean meadow remains in shallow brackish marshes or lagoons, submitted to wave action.

Facies with Munieria

This facies corresponds to group A facies (see Fig. 8f), including samples 13 and 19 (Fig. 7). In the field, these samples were sometimes found in top horizons of lacustrine cycles. They corresponded to light-colored grainstones overwhelmingly formed by remains of *Munieria grambasti* Bystrický 1976, a thallus probably related to charophytes as discussed above. This component may represent up to 70% of the total points counted. However, most of them (up to 50%) are small fragments, showing the characteristic crenulated external surface (Fig. 5b), which corresponds to the calcified intercellular space of *Munieria* internodes. Other skeletal components are extremely rare and include portions of thalli of genus *Charaxis*, clavatoracean utricles, porocharacean gyrogonites and ostracodes. This facies is attributed to the washed remains of a *Munieria grambasti* meadow on the shores of a shallow lake. The limited quantity of lime-mud and the co-occurrence of well-preserved internodes and abundant fragments are attributed to limited reworking before deposition. There were no marine or

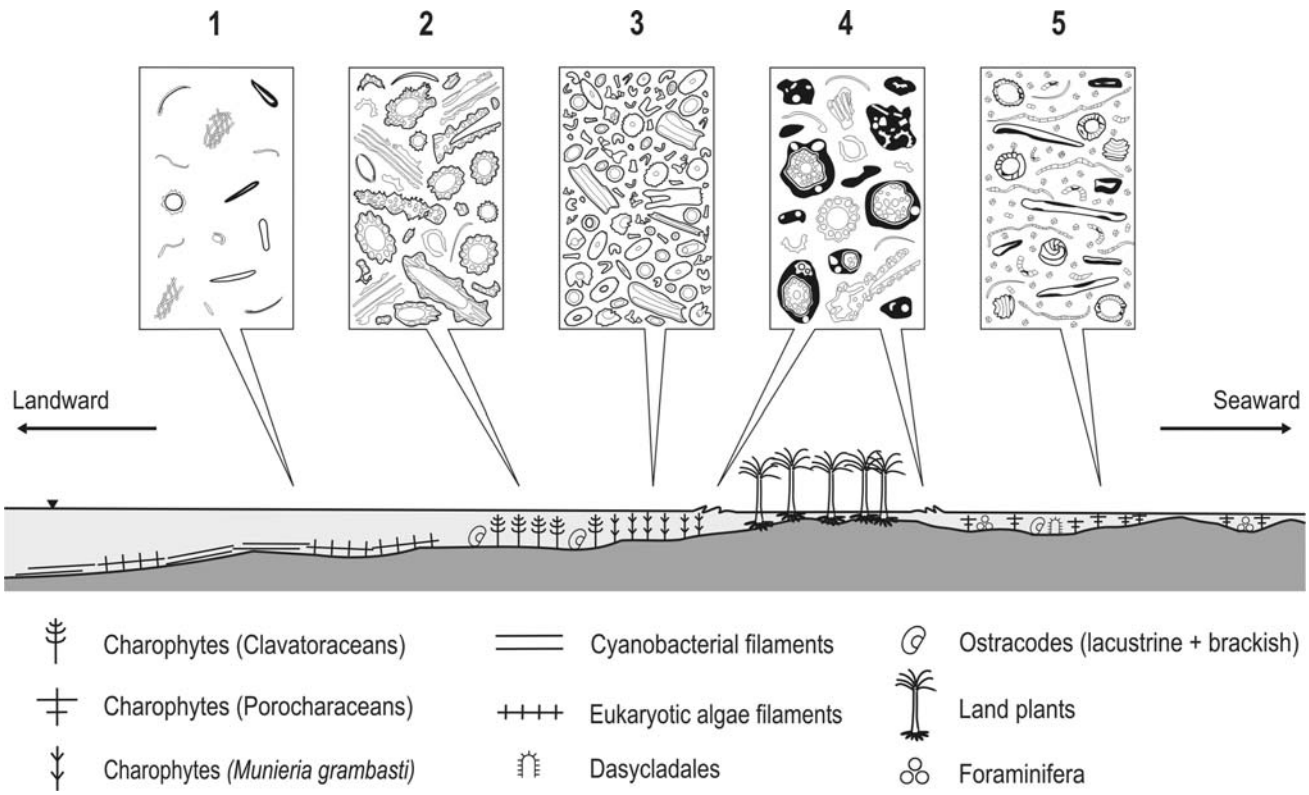

Fig. 9 Palaeoecological model for the non-marine Early Cretaceous of Creu del Vilar based on charophyte-rich microfacies. *1*. Microfacies of filamentous algae and clavatoraceans. Two sizes of filaments are represented, smaller filaments may form bundles (*Girvanella*). *2*. Microfacies of clavatoracean remains. Different sections of thalli of *Clavatoraxis, Charaxis*, clavatoracean utricles and ostracodes are shown. *3*. Microfacies with *Munieria*. Longitudinal, tangential and cross sections of *Munieria* are represented. *4*. Microfacies of charophyte remains and intraclasts. Both the intraclasts and the matrix contain abundant charophyte remains. Depending on the type of these remains, the freshwater or brackish condition of the palaeoenvironment can be determined. *5*. Microfacies of porocharacean remains. Sections of porocharacean gyrogonites, gyrogonite fragments, lituolid foraminifera and turtle eggshells are represented

brackish remains associated with *Munieria grambasti* Bystrický 1976, which suggests a freshwater habitat.

Discussion

The comparison of palaeontological results, including taxonomy, taphonomy and palaeoecology, with sedimentological analysis of the microfacies studied leads to the characterization of the depositional setting and the palaeoenvironment (Fig. 9). Most charophyte-rich microfacies from the Barremian of the Eastern Iberian Chain belong mainly to the freshwater domain (microfacies a, b, c, e); however, two microfacies are typical of brackish marshes and lagoons (microfacies c, d).

Microfacies and sedimentological analyses of samples from the freshwater domain appear to indicate a downslope zonation that is easy to characterize from the type and the preservation state of its different components. The samples include facies of filamentous algae and clavatoraceans in the deepest zone (Fig. 9.1), a belt of submerged vegetation made up of different charophyte meadows in the lake margins and finally the lakeshore belt made up of facies of charophyte remains and intraclasts (Fig. 9.4). The most diverse group of samples is represented by the facies attributed to charophyte meadows. An easy distinction was found between facies of clavatoracean remains (Fig. 9.2) and facies with *Munieria* (Fig. 9.3). Both types may include in situ or wave-reworked remains of charophyte meadows. The distinction between the two types is normally easy on the basis of taphonomic features such as good preservation/fragmentation of remains and the presence/absence of mud.

A second set of samples is related to brackish cycles. Brackish charophyte assemblages from the Tethyan Lower Cretaceous are characterized by homogeneous *Porochara* communities (Fig. 9.5), which are easily recognized in thin sections by their heavily calcified gyrogonites with an apical pore and presence of multipartite basal plates. As was the case with lacustrine assemblages, these remains may have been washed out, forming rocks poor in lime-mud and rich in gyrogonite fragments. The shores of brackish marshes show features comparable to the lakeshores, i.e., dominated by intraclasts and a few fragmentary charophyte remains (Fig. 9.4). However, in marshes, components show

clearly marine influence and are richer in porocharaceans, small benthic foraminifera and remains of other brackish or marine organisms.

These results provide evidence for a palaeoecological model based on charophyte-rich microfacies for the non-marine Lower Barremian of Creu del Vilar, Maestrat Basin, Eastern Iberian Chain (Fig. 9).

Conclusions

Five charophyte-rich microfacies were defined and interpreted in palaeoenvironmental terms in the Barremian of Creu del Vilar (Eastern Iberian Chain). These facies allowed us to characterize non-marine carbonate rocks on the basis of their skeletal components and to introduce valuable information and detail in the current facies analysis of non-marine depositional environments. The deepest parts of the lakes showed assemblages dominated by cyanobacterial filaments and fragments of clavatoracean thalli and utricles. The vegetation of lake margins consisted of charophyte meadows of different composition (clavatoracean meadows in most cases; and *Munieria* meadows in particular cases). In brackish environments, charophyte meadows were dominated by abundant porocharacean remains. The shores of lakes and marshes typically contain a facies with abundant intraclasts resulting from the reworking of the exposed sediments. Charophyte remains, associated with the matrix embedding intraclasts, enable lakeshores and shores of brackish marshes to be distinguished. The former contain abundant clavatoracean and other lacustrine remains, while the latter contain porocharacean remains.

Acknowledgements This study is a contribution to projects CGL2008-00809/BTE and CGL2008-04916/BTE of the Spanish Ministry of Science and Technology. We acknowledge the revision of the English text by Mr. Robin Rycroft (Servei d'Assessorament Lingüístic, Universitat de Barcelona). The original manuscript was improved by Ioan I. Bucur, Monique Feist, and André Freiwald during peer-review process.

References

Bystrický J (1976) *Munieria grambasti* sp. nov. in Kalk Gerölle der Upolav-Konglomerate des Mittleren Váh-Gebietes (Klippenzone, Westkarpaten). Geol Carpatica 27:45–64

Feist M, Grambast-Fessard N (1984) New porocharaceae from the Bathonian of Europe: phylogeny and palaeoecology. Palaeontology 27:295–305

Feist M, Génot P, Grambast-Fessard N (2003) Ancient Dasycladales and Charophyta: convergences and differences, with special attention to *Munieria baconica*. Phycol 42:123–132

Feist M, Grambast-Fessard N, Guerlesquin M, Karol K, Lu H, McCourt RM, Wang Q, Shenzen Z (2005) Treatise on invertebrate paleontology, Part B, Protoctista 1. Charophyta, vol 1. The Geological Society of America, Boulder

Flügel E (2004) Microfacies of carbonate rocks: analysis interpretation and application. Springer, Berlin

Grambast L (1966) Un nouveau type structural chez les Clavatoracées, son intérêt phylogénetique et stratigrafique. C R Séances Acad Sci Paris 262:1929–1932

Grambast L (1968) Evolution of the utricle in the charophyta genera *Perimneste* HARRIS and *Atopochara* PECK. J Linn Soc Bot 61:5–11

Grambast L (1969) La symétrie de l'utricule chez les Clavatoracées et sa signification phylogénétique. C R Acad Sci, Paris 269:878–881

Hammer Ø, Harper D (2006) Paleontological data analysis. Blackwell, Oxford

Martín-Closas C (2000) Els caròfits del Juràssic superior i Cretaci inferior de la Península Ibèrica. Arx Secc Ciènc Inst Est Catalans 125:1–304

Martín-Closas C (2003) The fossil record and evolution of freshwater plants. A review. Geol Acta 1:315–338

Martín-Closas C, Diéguez C (1998) Charophytes from the lower cretaceous of the Iberian ranges (Spain). Palaeontology 41:1133–1152

Martín-Closas C, Grambast-Fessard N (1986) Les charophytes du Crétacé inférieur de la région du Maestrat (Chaîne Ibérique, Catalanides, Espagne). Paléobiol Cont 15:1–66

Martín-Closas C, Clavel B, Schroeder R, Charollais J, Conrad MA (2009) Charophytes from the Barremian-lower Aptian of the Northern Subalpine Chains and Jura Mountains, France: correlation with associated marine assemblages. Cretaceous Res 30:49–62

Mojon PO (1989) Polymorphisme écophénotypique et paléoécologique des Porocharacées (Charophytes) du Crétacé basal (Berriasien) du Jura Franco-Suisse. Rev Paléobiol 2:505–524

Peck RE (1941) Lower Cretaceous Rocky Mountain non-marine microfossils. J Paleontol 15:285–304

Perrin C, Bosence DWJ, Rosen B (1995) Quantitative approaches to palaeozonation and palaeobathymetry of corals and coralline algae in Cenozoic reefs. In: Bosence DWJ, Allison PA (eds) Marine palaeoenvironmental analysis from fossils. Geol Soc London Spec Publ 83:181–229

Riding R (1991) Calcified cyanobacteria. In: Riding R (ed) Calcareous algae and stromatolites. Springer, Berlin

Riveline J, Berger JP, Bilan W, Feist M, Martín-Closas C, Schudack M, Soulié-Märsche I (1996) European Mesozoic–Cenozoic charophyte biozonation. Bull Soc Géol France 167:453–468

Salas R, Casas A (1993) Mesozoic extensional tectonics, stratigraphy and crustal evolution during the Alpine Cycle of the Eastern Iberian Basin. Tectonophysics 228:33–55

Salas R, Guimerà J, Mas R, Martín-Closas C, Meléndez A, Alonso A (2001) Evolution of the Mesozoic Central Iberian Rift System and its Cainozoic inversion (Iberian Chain). In: Ziegler PA, Cavazza W, Robertson AFH, Crasquin-Soleau S (eds) Peri-Tethys Memoir 6: PeriTethyan Rift/Wrench Basins and Passive Margins. Mém Mus Nat Hist Nat 186:145–185

Schudack ME (1993) Die Charophyten im Oberjura und Unterkreide Westeuropas Mit einer phylogenetischen Analyse der Gesamtgruppe. Berliner Geowissensch Abh A8:1–209

Wang Z, Lu H-N (1982) Classification and evolution of Clavatoraceae with notes on its distribution in China (in Chinese with English abstract). Bull Nanjing Inst Geol Palaeont Acad Sinica 4:77–104